Abnormal vascular architecture at the placental-maternal interface in preeclampsia

Justine Tack[2*], Carine Munaut[1*], Silvia Blacher[1], Agnès Noël[1], Michelle Nisolle[2], Frédéric Chantraine[2]

[1] Laboratory of Tumor and Developmental Biology, GIGA-R, University of Liège, Tour de Pathologie (B23), Sart Tilman, B-4000 Liège, Belgium
[2] Department of Obstetrics and Gynecology, University of Liège, Hôpital de la Citadelle, B-4000 Liège, Belgium. **Equally contributors*

ABSTRACT

Background and purpose: The aim of this study was to characterize the vascular architecture in the placental bed in pregnancies complicated by preeclampsia and in normal pregnancies.

Methods: Vessel numbers and cross-section area density in 11 preeclamptic placental beds were compared with 10 normal placental beds using computer-assisted image analysis of whole-slide CD31-immunolabeled sections.

Results: The total surface occupied by vessels was significantly reduced in preeclamptic placental beds compared with controls beds. However, the number of vessels/section and average surface were similar in all cases. Vessel size distribution differed between the two groups: more smaller vessels were found in preeclamptic placental beds.

Conclusions: Using a whole slide scanning and computer-assisted analysis method, we demonstrated a different morphological architecture of vessels in the placental beds of preeclamptic patients which might reflect the previously reported findings of insufficient trophoblast invasion and incomplete vascular remodeling.

KEYWORDS

Preeclampsia; placental bed, vessel architecture, virtual imaging.

Introduction

Preeclampsia (PE) is a pregnancy-associated disorder and a multisystem disease characterized by the sudden onset of hypertension associated with either proteinuria or end-organ dysfunction after 20 weeks of gestation in women with no previous history of hypertension. PE is one of the most important causes of maternal and perinatal morbidity and mortality, with PE-related deaths estimated to amount to 50,00-60,000 per year. The incidence of PE has increased by 25% in the United States over the past two decades [1].

The clinical manifestations are caused by mild to severe microangiopathy of different organs [2]. Hepatic or renal failure, pulmonary edema, cardiovascular disease and death are the potential maternal sequelae. On the fetal side, potential consequences of PE are late miscarriage, retro-placental hematoma, fetal growth restriction (FGR), hypoxic neurologic injury and in utero fetal death. These fetal and neonatal consequences result from placental hypoperfusion.

Several genetic, immunologic, physiological, environmental, demographic and pregnancy-associated factors have been associated with the occurrence of PE. These include: multiple pregnancy, maternal age at the extremes of the fertile range, personal and family history of PE, obesity, ethnic group, egg donation, chronic hypertension, renal disease, metabolic disease and thrombophilia [3,4].

Although the etiology of PE has not been completely elucidated, the placenta plays a central role in the development of this disease. The prevailing view, supported by epidemiologic and experimental data, is that PE is due largely to a defect in trophoblast invasion and the remodeling of the uterine spiral arteries [5]. It results in impaired placentation in the first trimester of pregnancy, leading to inadequate placental perfusion in the second and third trimesters [6]. This process leads to an imbalance between pro-angiogenic and anti-angiogenic factors, released by the placenta into the maternal circulation, that causes systemic endothelial dysfunction [7]. However, a precise definition of the vascular architecture at the placental-maternal interface is lacking in women with PE.

The aim of this study was to characterize the vascular architecture in the placental bed in pregnancies complicated by PE and in normal pregnancies, applying our previously published method consisting of high-resolution virtual imaging of whole-tissue sections and computer-assisted image analysis of the placental bed of PE patients and controls [8].

Article history
Received 15 Mar 2019 - Accepted 25 Oct 2019

Contact
Carine Munaut; c.munaut@ulg.ac.be
Tel: +32 4 366 24 53
Fax: +32 4 366 29 36

Methods

Tissue collection

The American College of Obstetricians and Gynecologists (ACOG) defines PE as the onset, after 20 weeks of amenorrhea,

of hypertension (≥ 140/90) associated with proteinuria and/or single or multiple organ involvement [9]. Placental bed biopsies were obtained prospectively from 11 patients presenting PE and from 10 women presenting uncomplicated pregnancies and delivered by elective cesarean section for breech presentation, feto-pelvic disproportion or a history of two previous cesarean sections. All these biopsies were sampled under direct vision by the same operator (F.C.); samples were obtained after placental delivery from the central zone of the placental site applying the previously described knife technique [10,11]. Adequacy of the samples was controlled by analysis of hematoxylin-eosin–stained sections. Only areas in which myometrium was present were analyzed. These placental bed biopsies were analyzed by two operators (F.C. and J.T.).

Histology and immunohistochemistry

All biopsies were fixed in 4% formaldehyde in phosphate-buffered saline (PBS) and embedded in paraffin. Immunohistochemistry for CD31 (vascular endothelial cell marker) was performed on 4-µm thick paraffin sections that were mounted on aminopropyltriethoxysilane (Tespa)-coated glass slides.

The sections were dewaxed in xylene and rehydrated. Antigen retrieval was achieved using Target Retrieval Solution (S2031; DakoCytomation, Glostrup, Denmark). Endogenous peroxidases were blocked by incubation in 3% H2O2 for 20 minutes, and nonspecific binding was prevented by incubation in PBS/normal goat serum. Sections were incubated with monoclonal anti-CD31 (M0823, 1:40; DakoCytomation) for 60 minutes at 37°C and then biotinylated goat antimouse IgG (E0433, 1:400; DakoCytomation), followed by streptavidin/horseradish peroxidase (P0397, 1:500; DakoCytomation).

Labeling was visualized with 3-3-diaminobenzidine hydrochloride (K3468; DakoCytomation) as the chromogen and hematoxylin as the counterstain. Nonspecific binding of primary antibody was evaluated using mouse IgG1 at the same immunoglobulin concentration as the primary antibody (X0931; DakoCytomation).

Image acquisition, processing, and measurements

Virtual images of the whole tissue sections were acquired using the fully automated digital microscopy system dot-Slide (BX51TF; Olympus, Aartselaar, Belgium) coupled with a Peltier-cooled, high-resolution digital color camera (XC10; Olympus) at a resolution of 1376 x 1032 pixels. Whole-tissue sections at high magnification (x100) were scanned, yielding virtual images with a 0.65 µm pixel size.

The vessel parameters were characterized in the myometrium located under the placental-myometrial junction. Binary images were decimated before quantification, according to a previously described procedure because the original virtual images exceeded several gigabytes. CD31-identified endothelial cells allowed automatic computerized acquisition of blood vessel characteristics. Vessel area density was defined as the number of pixels belonging to all vessels (endothelium and encompassed lumen, i.e., the total area occupied by vessels) divided by the total number of pixels of the myometrial area. The number of vessel cross-sections per unit area was defined as the number of vessels divided by the area of myometrium. The area of each vessel cross-section was measured, and the vessel cross-section area distribution was plotted as a histogram. Image processing and measurements were performed using MATLAB version 9.2 software (MathWorks, Natick, MA).

Statistical analysis

The results are expressed as means ± 95% CI of individually tested parameters (vessel area density, number of vessels/unit area, area of individual vessel sections, vessel cross-section area distribution, and distance from each vessel to the placental-myometrial junction) (Table 1). For each parameter, a large number of measurements was performed in each individual (mean number of vessels per tissue section, 3385 ± 850.8 for PE cases and 2863 ± 466.5 for control cases). Tests of homogeneity performed in each group (PE and control) confirmed the homogeneity of both populations for the evaluated parameters. It can therefore be concluded that for the tested parameters, the PE and the control group displayed homogenous characteristics. The statistical differences between the groups were assessed using the nonparametric Mann-Whitney U test. Furthermore, we used the nonparametric Kolmogorov-Smirnov test for distributions and analysis of covariance for linear regressions. $P < 0.05$ defined significance. Statistical analyses were performed with MATLAB version 9.2 software.

Results

Table 2 summarizes the demographic and obstetric characteristics of the PE patients and controls. There was no significant difference in gravidity and parity between the two groups. As expected, women with PE had higher blood pressure and abnormal proteinuria. Furthermore, the women with PE delivered significantly earlier than the controls.

Table 1

	VESSEL SURFACE DENSITY		NUMBER OF SECTIONS		AVERAGE SURFACE	
	CT	PE	CT	PE	CT	PE
Mean	0,09694	0,06079	80,13	64,9	0,001453	0,000962
SD	0,05303	0,01903	50,54	16,03	0,000662	0,000309
SEM	0,01677	0,005738	15,98	4,833	0,000209	9,31E-05
Lower 95% CI of mean	0,05901	0,04801	43,98	54,14	0,00098	0,000754
Upper 95% CI of mean	0,1349	0,07358	116,3	75,67	0,001927	0,001169

Table 1 Demographic and obstetrical characteristics.

VARIABLE	CONTROLS (N=10)	PREECLAMPSIA (N=11)	*P* VALUE
Maternal age at delivery (years)[a]	29 (20- 42)	28 (23- 38)	NS
Gestational age at delivery (weeks)[a]	38.5 (32.7-39)	32 (25.3- 37.1)	0,00003
Gravidity[a]	3 (1-8)	3 (1-6)	NS
Parity[a]	2 (0-7)	1 (0-2)	NS
HELLP	0/10	3/11	
Proteinuria	0/10	10/11	
Systolic BP (mmHg)	121 (101-155)	145 (125-185)	0,021
Diastolic BP (mmHg)	72.8 (62-105)	88.18 (71-105)	0,032
Birth weight (g)	3240 (1660-3838)	1540 (480- 2258)	0,0004

NS, not significant. [a] Data presented are expressed in medians (minimum-maximum) and analyzed with the Mann-Whitney U test

Figure 1 illustrates the computer-assisted image algorithm for a control and a PE case. On the whole-slide section most vessels were automatically detected, whereas some missed vessels and the limits of tissue section were manually corrected. Figure 1 (B and E) shows binarized images, subsequently used for vascular architecture characterization.

Placental bed vessel characteristics

The mean number of vessels per tissue section was similar in the control and PE groups (80.13 ±0.13 vessels/mm^2 vs 64.90 ± 4.83 vessels/mm^2, *P*= 0.8053, figure 2A). However, in the PE group the cross-sectional vessel areas were reduced compared with what was observed in the control group (0.0608 ± 0.0057 vs 0.0969 ± 0.0168, *P*= 0.0378, figure 2B). The surface occupied by blood vessels was determined and found to be slightly reduced in PE (0.0962 10^{-3} ± 0.0932 10-3 vessels/mm^2 vs 1.453 10^{-3} ± 0.294 10^{-3} vessels/mm^2, *P*=0.0620, figure 2C). To confirm this, the $\log_{10}$ –transformed vessel size distribution was analyzed (Figure 2D). This normalized histogram indeed highlights the presence of smaller vessels in PE.

Discussion

In this study, we compare the vessel organization in the placental bed of PE cases compared with the placental bed in normal pregnancy applying a method previously used by our workgroup to describe vascular characteristics in early invasive cervical cancer and placenta increta [8,12]. This method combines the use of a high-resolution virtual imaging system on whole-tissue sections with the use of computer-assisted image analysis of whole-slide CD31-immunolabeled sections. Through this method, we demonstrated and confirmed that more smaller vessels are present in PE placental beds compared with normal placental beds.

PE is a complex disorder with a large range of clinical pres-

Figure 1 Illustration of the computer-assisted image analysis of vessels in control sections (A-C) and PE sections (D-F). A and D, representative CD31-positive immunolabeled vessels. B and E, binarized images generated from from immunolabeled sections. C and F, selected zones at higher magnification. Figure 1G shows a close up of the CD31 staining.

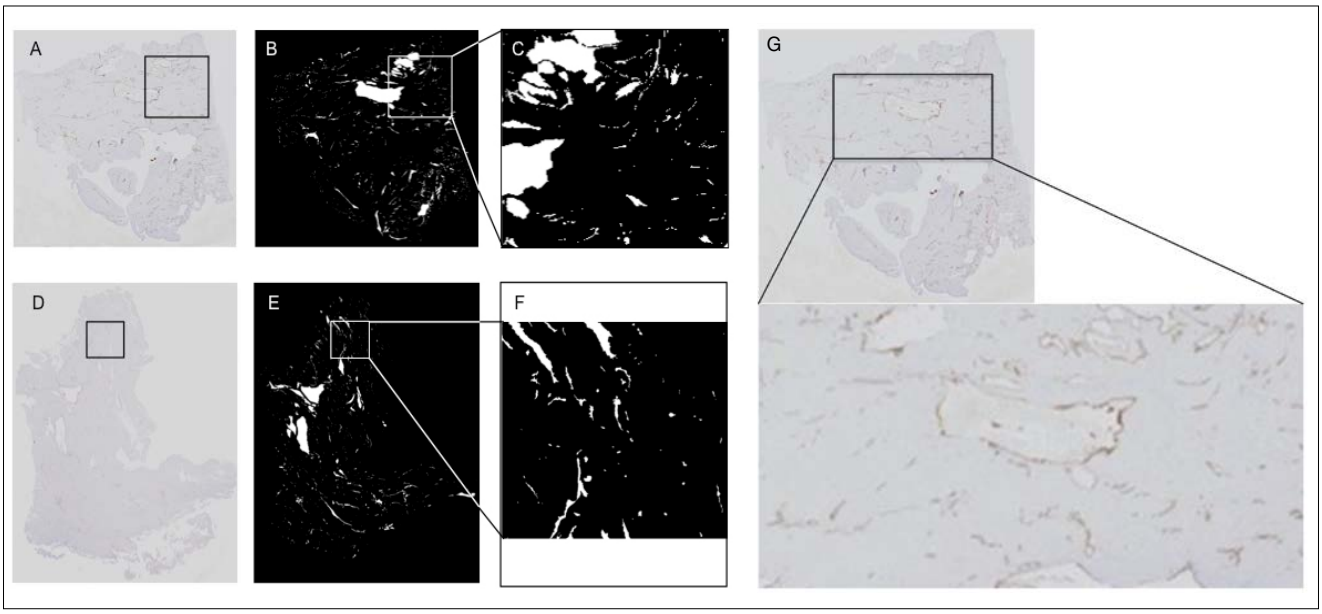

Figure 2 A, Mean number of vessels per cross-section. B, Vessel area density. C, Mean vessel cross-section area. D, Histogram of the normalized frequency of vessels versus vessel cross-section area distribution (log_{10} scale).

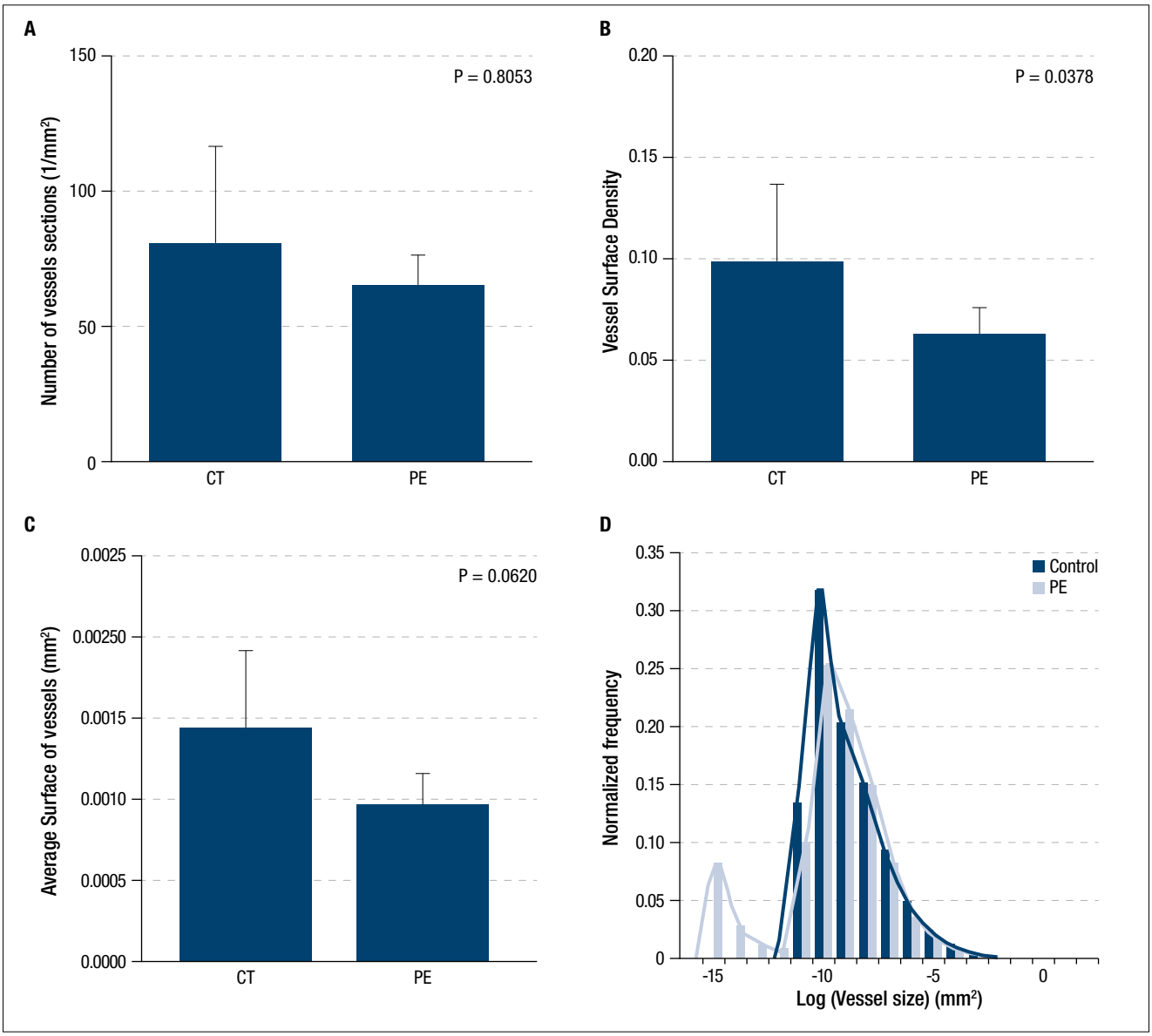

entations. This heterogeneity suggests the possible existence of various pathogenic mechanisms. It is well known that PE is associated with poor placentation and incomplete remodeling of the utero-placental spiral arteries [13].

Despite extensive study of the pathogenesis of PE, the exact vascular architecture of the placental bed in PE is unclear. As regards the placenta, increased villous capillary branching has been reported in placentas from PE versus normal term pregnancies [14]. In contrast, other investigators have reported decreased micro-vessel counts in PE placentas [5, 15, 16] or unchanged vascular densities between PE and normal term placentas [17, 18]. As early as 1985, Las Heras *et al*. showed a significant reduction in the *ratio* of lumen-to-whole-diameter of the fetal arteries in "toxemia" as compared with normal pregnancy and acute fetal distress groups [19]. Moreover, they showed that the mean lumen-to-whole-diameter *ratio* also differed between regions of the placenta in all groups, the most marked reduction being in the parachorial region and the least prominent reduction in the parabasal zone. Finally, they found no significant differences in the mean diameter *ratio* between three subgroups of the toxemic pregnancies (PE, essential hypertension and renal disease groups).

More recently, Uras *et al*. evaluated placentas of PE cases by using immuno-histochemical staining with CD31 and with Factor VIII antibodies. When the PE and control groups were compared, CD31 and Factor VIII staining were significantly lower in the PE group. This study indirectly suggests that the balance between proangiogenic and antiangiogenic factors is shifted in favor of anti-angiogenic factors in PE [15].

In 2013, Lyall *et al*. demonstrated the occurrence of a major defect in myometrial spiral artery remodeling in PE [5]. In this study, placental bed biopsies were immuno-stained to determine vessel wall integrity, extravillous cytotrophoblast location/density, periarterial fibrinoid, and endothelium. The authors compared normal pregnancies and pregnancies complicated by PE or severe FGR and they examined spiral artery

remodeling and extravillous cytotrophoblast density. The invasion of vessel wall smooth muscle was reduced in myometrial spiral arteries in PE and FGR groups compared with controls. Although failure to destroy myometrial vessel wall smooth muscle is a feature of PE, 10% of decidual vessels in PE also retained their muscle wall. Moreover, interstitial extravillous cytotrophoblast density seems to be similar in normal pregnancy and PE and the normal group showed more intramural extravillous cytotrophoblasts than the PE group. This work suggests that lack of intramural trophoblasts in the myometrial vessels rather than defective interstitial trophoblast invasion may be the primary abnormality in PE [20]. In our study, we focused on the size and the areas occupied by vessels. We did not perform detailed analysis of the histologic appearance of the different vessels in the placenta beds.

Possible limitations of this study are the small sample size and the two-observer analysis. Moreover, another possible limitation is the difficulty in collecting gestational age matched bed biopsies from normal pregnancies as controls. However, the median 5-week difference in gestational length between our groups should not drastically affect vessel size and distribution in the placental bed. We chose patients undergoing elective term cesarean section deliveries as the control group in order to obtain placental bed biopsies of good quality and to avoid the bias of impaired placentation in earlier deliveries often indicated for pregnancies complicated by PE, intrauterine growth restriction (IUGR) or premature rupture of membranes.

This study confirms previously published data on placental bed abnormality in pregnancies complicated by PE. In this clinical situation, vessels are smaller in size, which can explain the under-perfusion of the placenta. Compared with manual or stereotaxic methods, the automated detection of CD31-stained histologic sections used in this study allows easier and probably more precise measurement of the number and size of vessels.

Conclusion

Through whole slide scanning and computer-assisted analysis, we revealed a different morphological architecture of vessels in the placental bed in PE. This might reflect the insufficient trophoblast invasion and incomplete vascular remodeling previously described by others.

References

1. Hypertension in pregnancy. Report of the American College of Obstetricians and Gynecologists' Task Force on Hypertension in Pregnancy. Obstet Gynecol. 2013; 122: 1122-31.
2. Stella CL, Sibai BM. Preeclampsia: Diagnosis and management of the atypical presentation. J Matern Fetal Neonatal Med. 2006; 19: 381-6.
3. Pare E, Parry S, McElrath TF, Pucci D, Newton A, Lim KH. Clinical risk factors for preeclampsia in the 21st century. Obstet Gynecol. 2014;124: 763-70.
4. Emonts P, Seaksan S, Seidel L, Thoumsin H, Gaspard U, Albert A, et al. Prediction of maternal predisposition to preeclampsia. Hypertens Pregnancy. 2008; 27: 237-45.
5. Lyall F, Robson SC, Bulmer JN. Spiral artery remodeling and trophoblast invasion in preeclampsia and fetal growth restriction: relationship to clinical outcome. Hypertension. 2013; 62: 1046-54.
6. Fisher SJ. Why is placentation abnormal in preeclampsia? Am J Obstet Gynecol. 2015; 213: S115-22.
7. Foidart JM, Schaaps JP, Chantraine F, Munaut C, Lorquet S. Dysregulation of anti-angiogenic agents (sFlt-1, PLGF, and sEndoglin) in preeclampsia--a step forward but not the definitive answer. J Reprod Immunol. 2009; 82: 106-11.
8. Chantraine F, Blacher S, Berndt S, Palacios-Jaraquemada J, Sarioglu N, Nisolle M, et al. Abnormal vascular architecture at the placental-maternal interface in placenta increta. Am J Obstet Gynecol. 2012; 207: 188 e1-9.
9. American College of Obstetricians and Gynecologists; Task Force on Hypertension in pregnancy. Hypertension in pregnancy. Report of the American College of Obstetricians and Gynecologists' task force on hypertension in pregnancy. Obstet Gynecol. 2013;122:1122-31.
10. Robertson WB, Khong TY, Brosens I, De Wolf F, Sheppard BL, Bonnar J. The placental bed biopsy: review from three European centers. Am J Obstet Gynecol. 1986; 155: 401-12.
11. Veerbeek JHW, Post Uiterweer ED, Nikkels PGJ, Koenen SV, van der Zalm M, Koster MPH, et al. Biopsy techniques to study the human placental bed. Placenta. 2015; 36: 775-82.
12. Balsat C, Blacher S, Signolle N, Beliard A, Munaut C, Goffin F, et al. Whole slide quantification of stromal lymphatic vessel distribution and peritumoral lymphatic vessel density in early invasive cervical cancer: a method description. ISRN Obstet Gynecol. 2011; 2011: 354861.
13. Pijnenborg R, Vercruysse L, Hanssens M. The uterine spiral arteries in human pregnancy: facts and controversies. Placenta. 2006; 27: 939-58.
14. Boyd PA, Scott A. Quantitative structural studies on human placentas associated with pre-eclampsia, essential hypertension and intrauterine growth retardation. Br J Obstet Gynaecol. 1985; 92: 714-21.
15. Uras N, Oguz SS, Zergeroglu S, Akdag A, Polat B, Dizdar EA, et al. CD31 and Factor VIII in angiogenesis of normal and pre-eclamptic human placentas. J Obstet Gynaecol. 2012; 32: 533-6.
16. Brosens I, Pijnenborg R, Vercruysse L, Romero R. The "Great Obstetrical Syndromes" are associated with disorders of deep placentation. Am J Obstet Gynecol. 2011; 204: 193-201.
17. Burton GJ, Woods AW, Jauniaux E, Kingdom JC. Rheological and physiological consequences of conversion of the maternal spiral arteries for uteroplacental blood flow during human pregnancy. Placenta. 2009; 30: 473-82.
18. Li Y, Zhao YJ, Zou QY, Zhang K, Wu YM, Zhou C, et al. Preeclampsia does not alter vascular growth and expression of CD31 and vascular endothelial cadherin in human placentas. J Histochem Cytochem. 2015; 63: 22-31.
19. Las Heras J, Baskerville JC, Harding PG, Haust MD. Morphometric studies of fetal placental stem arteries in hypertensive disorders ('toxaemia') of pregnancy. Placenta. 1985; 6: 217-27.
20. Burke SD, Karumanchi SA. Spiral artery remodeling in preeclampsia revisited. Hypertension. 2013; 62: 1013-4.

Acknowledgements: *The authors thank E. Feyereisen and I. Dasoul for their excellent technical assistance.*
The authors thank the Fonds de la Recherche Scientifique - FNRS (F.R.S.-FNRS, Belgium), the Fonds spéciaux de la Recherche (University of Liège), the Fonds Léon Fredericq (University of Liège), the Direction Générale Opérationnelle de l'Economie, de l'Emploi et de la Recherche from the Service Public de Wallonie (SPW, Belgium).
Funding: *This work was supported by grants from the Fonds de la Recherche Scientifique - FNRS (F.R.S.-FNRS, Télévie, Belgium) and the Fonds Léon Fredericq (University of Liège)*